Interplay between spin-density-wave and superconducting states in quasi-one-dimensional conductors

R. Duprat and C. Bourbonnais[a]

Centre de Recherche sur les Propriétés Électroniques de Matériaux Avancés, Département de Physique, Université de Sherbrooke, Sherbrooke, Québec, J1K 2R1, Canada

Abstract. The interference between spin-density-wave and superconducting instabilities in quasi-one-dimensional correlated metals is analyzed using the renormalization group method. At the one-loop level, we show how the interference leads to a continuous crossover from a spin-density-wave state to unconventional superconductivity when deviations from perfect nesting of the Fermi surface exceed a critical value. Singlet pairing between electrons on neighboring stacks is found to be the most favorable symmetry for superconductivity. The consequences of non uniform spin-density-wave pairing on the structure of phase diagram within the crossover region is also discussed.

PACS. 71.10.Li Excited states and pairing interactions in model systems – 74.20.Mn Nonconventional mechanisms (spin fluctuations, polarons and bipolarons, resonating valence bond model, anyon mechanism, marginal Fermi liquid, Luttinger liquid, etc.) – 74.70.Kn Organic superconductors

1 Introduction

The problem raised by the interdependence of antiferromagnetism and superconductivity in low dimensional electronic materials stands among the most important challenges facing condensed matter physics in the last two decades or so. Although this issue takes on considerable importance in the description of high-temperature cuprate superconductors [1–3], it likely acquired its first focus of interest in the context of quasi-one-dimensional organic superconductors, the Bechgaard salts [(TMTSF)$_2$X] and their sulfur analogs, the Fabre salts [(TMTTF)$_2$X]. The close proximity of antiferromagnetic correlations with the onset of organic superconductivity in the temperature and pressure phase diagram of these compounds soon indicated that the apparent difficulty of describing both phenomena could originate in their mutual interaction [4–6].

Given the dominant part played by Coulomb repulsion on the scene of interactions in these materials [7], early attempts to consider the nature of superconducting pairing suggested that in order to avoid local repulsion — so resistant to conventional pairing [5] — electrons may pair on different stacks [8]. The driving force for such a pairing would derive from antiferromagnetic spin fluctuations [4,5], a mechanism that can be seen as the spin counterpart of what Kohn and Luttinger have proposed long ago for pairing induced by charge (Friedel) oscillations in

the context of isotropic metals [9]. Its influence in quasi-one-dimensional metals, however, turns out to be more important than in isotropic materials extending over a larger domain of temperature in the normal phase [10,11], and becoming further enhanced by singular spin-density-wave (SDW) correlations near the critical pressure P_c above which superconductivity (SC) is singled out as the only stable state. An intrinsic difficulty of this problem is that both SDW and SC instabilities refer to the same electron degrees of freedom. Put at the level of elementary scattering events close to the Fermi surface, electron-hole pairs leading to density-wave correlations interfere with the electron-electron (hole-hole) pairs connected with superconductivity. In previous ladder diagrammatic summation [5,7,10,12], mean-field [13,14] and RPA [15,16] approaches to ordered phases at low temperature, interference is neglected; an assumption actually grounded on the existence of a coherent warped Fermi surface which is considered as sufficient to entirely decouple both types of pairing so that each can be treated separately in perturbation theory [17]. However, as the electron system deconfines at low temperature, namely when a Fermi liquid component can be defined in at least two spatial directions, interference — of maximum strength in the 1D non-Fermi (Luttinger) liquid domain — is still present for quasiparticles but becomes non uniform along the open Fermi surface. It turns out that it is precisely from this uneven pairing that the interplay between SDW and SC states is found to take place. In practice, the treatment of

[a] e-mail: `cbourbon@physique.usherb.ca`

both singularities using the renormalization group (RG) method proved not insurmountable if interactions within the Fermi liquid component are not too large and a reduction of the number of momentum variables in flow equations can be made. Thus at the one-loop RG level, we will show that when density-wave and superconducting channels interfere on equal footing [18], the Kohn-Luttinger mechanism is dynamically generated from which a critical threshold for nesting deviations lead to a SDW-SC crossover, a feature that underlies the possibility of reentrant superconductivity, in fair agreement with experimental findings for $(TM)_2X$ materials in general [19,20]. As far as the nature of superconductivity is concerned, singlet interchain pairing is found to be the most favoured symmetry of this ordered state [21].

In Section 2, we introduce the model and define the effective theory for interacting quasi-particles at low energy. The renormalization group method is applied in Section 3 and flow equations for the scattering amplitudes are found. The possibilities of long-range order in either density-wave (Peierls) or superconducting (Cooper) channel are then analyzed as a function of deviations from perfect nesting of the Fermi surface. The results for the couplings are corroborated by the evaluation of the response functions in both channels. We close the Section 3 with considerations on the possibility of reentrant superconductivity in the crossover region. Concluding remarks are given in Section 4.

2 The model at low energy

We shall base our theoretical description of the competition between antiferromagnetism and superconductivity on the quasi-one-dimensional electron gas model. Consider a system of interacting electrons in a linear array of $N_\perp$ chains of length L (the interchain distance $d_\perp = 1$) and described by the Hamiltonian

$$H = H_0 + H_I = \sum_{p,\mathbf{k},\sigma} E_p(\mathbf{k})\, a^\dagger_{p,\mathbf{k},\sigma} a_{p,\mathbf{k},\sigma}$$

$$+ (LN_\perp)^{-1} \pi v_F \sum_{\{\mathbf{k},\mathbf{q},\sigma\}} (g_2 \delta_{\sigma_1\sigma_4}\delta_{\sigma_2\sigma_3} - g_1 \delta_{\sigma_1\sigma_3}\delta_{\sigma_2\sigma_4})$$

$$\times\, a^\dagger_{+,\mathbf{k}_1+\mathbf{q},\sigma_1} a^\dagger_{-,\mathbf{k}_2-\mathbf{q},\sigma_2} a_{-,\mathbf{k}_2,\sigma_3} a_{+,\mathbf{k}_1,\sigma_4}, \quad (1)$$

where

$$E_p(\mathbf{k}) = \epsilon_p(k) - 2t_\perp \cos k_\perp - 2t_{\perp 2}\cos 2k_\perp, \quad (2)$$

is the electron spectrum, while $\epsilon_p(k) = v_F(pk - k_F^0)$ is the one-dimensional − linearized − part of the spectrum close to the left and right Fermi points $pk_F^0 = \pm k_F^0$ and v_F is the 1D Fermi velocity [$\mathbf{k} \equiv (k, k_\perp)$]. The interchain single electron hopping $t_\perp$ is considered as small compared to the Fermi energy $E_F = v_F k_F^0$ ($\hbar = 1$), which is fixed to be half of the bandwidth cut-off $E_0 \equiv 2E_F$ along the chains. The even smaller transverse hopping term to second nearest-neighbor chains $t_{\perp 2} \ll t_\perp$ is included in order to parametrize nesting deviations of the entire Fermi surface. As for the interacting part H_I, we follow the usual 'g-ology' decomposition of the direct interaction between carriers defined close to the 1D Fermi points and retain the backward g_1 and forward g_2 scattering amplitudes − here normalized by πv_F − between right- and left-moving carriers [22]. Given the metallic conditions, one can take into account of the influence of umklapp scattering through a renormalization of g_2 at low energy [6,7,23,24].

In the following, we will examine the properties of the model in the gapless regime at sufficiently low energy scale, that is when a coherent interchain motion for electrons prevails and a Fermi liquid component can be defined. More specifically, we will focus on the effective Hamiltonian or − which will be more convenient for our purposes − on the effective action of the system having $E_x \ll E_0$ as a new bandwidth cut-off for electrons in the neighborhood of an open but warped Fermi surface. This corresponds to the temperature domain $T < E_x/2$ ($k_B = 1$) of transverse coherence at the single-particle level [25]. Application of the RG method in the 1D energy domain allows the systematic integration of high-energy degrees of freedom [25]. The resulting partition function for our model can then be expressed as a functional integral

$$Z = \text{Tr}\, e^{-\beta H}$$
$$\sim \iint_< D\psi^* D\psi\, e^{S^*[\psi^*,\psi]} \quad (3)$$

over the fermion fields ψ having energies below E_x. In the Fourier-Matsubara space, the essential contributions to the effective action S^* − up to a renormalization factor for the fields − can be written in the form

$$S^*[\psi^*,\psi] = S_0^*[\psi^*,\psi] + S_I^*[\psi^*,\psi]$$

$$= \sum_{p,\sigma}\sum_{\{\tilde{\mathbf{k}}\}^*} [G_p^0(\tilde{\mathbf{k}})]^{-1}\, \psi^*_{p,\sigma}(\tilde{\mathbf{k}})\psi_{p,\sigma}(\tilde{\mathbf{k}})$$

$$- \pi v_F \sum_{\mu,\tilde{\mathbf{Q}},} J_\mu(q_\perp,\ell_x) O^*_\mu(\tilde{\mathbf{Q}})O_\mu(\tilde{\mathbf{Q}}) + \dots, \quad (4)$$

where

$$G_p^0(\tilde{\mathbf{k}}) = [i\omega_n - E_p^*(\mathbf{k})]^{-1}, \quad (5)$$

is the 'free' propagator in which the substitutions $t_{\perp(2)} \to t^*_{\perp(2)} < t_{\perp(2)}$ lead to the renormalization of the spectrum $E_p \to E_p^*$ [here $\tilde{\mathbf{k}} = (\mathbf{k}, \omega_n = \pm\pi T, \pm 3\pi T, \dots)$]. The cut-off $E_x \approx t_\perp^*$ fixes the maximum energy (or twice the maximum temperature) and the range $\{\mathbf{k}\}^*$ of wavevectors in the deconfined region. The right (resp. left) warped open Fermi surface is parametrized by $k_\perp$

$$k_F(k_\perp) = \pm\left(k_F^0 + 2\frac{t_\perp^*}{v_F}\cos k_\perp + 2\frac{t_{\perp 2}^*}{v_F}\cos 2k_\perp \right). \quad (6)$$

It is convenient to write the effective interaction between electrons denoted S_I^* in (4) as products of electron-hole

pair fields

$$O_\mu(\tilde{\mathbf{Q}}) = \sqrt{\frac{T}{LN_\perp}} \sum_{\alpha,\beta\{\tilde{\mathbf{k}}\}^*} \psi^*_{-,\alpha}(\tilde{\mathbf{k}} - \tilde{\mathbf{Q}})\,\sigma_\mu^{\alpha\beta}\,\psi_{+,\beta}(\tilde{\mathbf{k}}) \quad (7)$$

describing CDW ($\mu = 0$) and SDW ($\mu = 1, 2, 3$) correlations, where σ_0 and $\sigma_{1,2,3}$ are the identity and Pauli matrices respectively [$\tilde{\mathbf{Q}} = (2k_F^0 + q, q_\perp, \omega_m = 0, \pm2\pi T, \dots)$, $q \ll 2k_F^0$]. These correlations are associated to the combinations of couplings

$$J_{\mu=0}(q_\perp, \ell_x) = -\frac{1}{2}(g_2^* - 2g_1^*) + j_{\perp 0}\cos q_\perp,$$
$$J_{\mu\neq0}(q_\perp, \ell_x) = -\frac{1}{2}g_2^* + j_{\perp\mu}\cos q_\perp, \quad (8)$$

for the CDW and SDW amplitudes respectively, where the g_i^* are the renormalized intrachain couplings evaluated at ℓ_x ($E_x = E_0 e^{-\ell_x}$). The $q_\perp$ dependence comes from the interchain short-range correlations that are generated in the 1D energy interval from the combined influence of g_i and $t_\perp$, that is from E_0 down to E_x. The corresponding interchain pair hopping amplitudes denoted $j_{\perp\mu}$, follow from an explicit RG calculation and then modify the boundary conditions for the low-energy description [25]. J_μ is taken independent of the longitudinal momentum and Matsubara frequency which is irrelevant (in the RG sense) in the 1D domain. This independence is assumed to carry over at lower energy as implied for example in the k-dependence of boundary conditions (8), where the couplings defined with respect to 1D Fermi points are used to describe scattering events on energy edges $\pm E_x/2$ with respect to a warped Fermi surface.

3 Interference between density-wave and superconductivity

The nature of correlations that can naturally develop in the deconfined region for electrons is linked in the first place to the amplitude and sign of J_μ. For repulsive couplings $g_{1,2} > 0$, the SDW coupling ($\mu \neq 0$) is negative and the most favorable, while the CDW one, though potentially of the right sign, is sizably weaker in amplitude at $T > E_x/2$. In the second place, the possibility for these correlations to develop long-range order at lower temperature is bound to the singular (logarithmic) response of the system to produce staggered density-wave correlations; it relies on the electron-hole symmetry of the spectrum, that is on nesting properties. For an open Fermi surface, however, the singular response to electron-hole pairing, albeit weakened by $t_{\perp 2}$, competes with the response of the Cooper channel for electron-electron pairing, which is also singular and unaltered by nesting deviations.

3.1 One-loop renormalization group

The summation of the leading interfering contributions of the perturbation theory below E_x is best obtained from

the application of the RG method. The technique consists in partial integrations of Z over fermion degrees of freedom denoted as $\bar{\psi}^{(*)}$ in the outer energy shell (o.s) $\pm E_x(\ell)d\ell/2$ above and below the warped Fermi surface [25], where $E_x(\ell) = E_x e^{-\ell}$ with $\ell > 0$, is now the scaled bandwidth below E_x. Focusing on the results at the one-loop level, we have

$$Z \sim \iint_< D\psi^* D\psi\, e^{S^*[\psi^*,\psi]_\ell} \iint_{o.s} D\bar{\psi}^* D\bar{\psi}\, e^{S_0^*}\, e^{S_{I,2}^* + \cdots}$$
$$\propto \iint_< D\psi^* D\psi\, e^{S^*[\psi^*,\psi]_\ell} + \frac{1}{2}\langle S_{I,2}^{*2}\rangle_{o.s} + \cdots \quad (9)$$

where $\langle(S_{I,2}^*)^2\rangle_{o.s}$ are the one-loop outer energy shell averages calculated with respect to $S_0^*[\bar{\psi}^*, \bar{\psi}]$, which ultimately lead to the renormalization (flow) of the J_μ couplings in S as a function of ℓ. Explicitly, by taking $S_{I,2}^*$ as a decomposition of the interaction having two fields among four to be contracted in the outer shell and retaining the contributions coming from the Peierls and Cooper channels, one finds

$$S_{I,2}^* = S_{I,2}^P + S_{I,2}^C$$
$$= -\pi v_F \sum_\mu \sum_{\tilde{\mathbf{k}}} \sum_{\{\tilde{\mathbf{k}}',\tilde{\mathbf{Q}}\}^*} J_\mu(q_\perp - k_\perp', k_\perp'; \ell)$$
$$\times \bar{O}_\mu^*(\tilde{\mathbf{k}} - \tilde{\mathbf{Q}}_0)\, O_\mu(\tilde{\mathbf{k}}' - \tilde{\mathbf{Q}}) + \text{c.c}$$
$$+ \pi v_F \sum_{\bar{\mu}} \sum_{\tilde{\mathbf{k}}} \sum_{\{\tilde{\mathbf{k}}',\tilde{\mathbf{Q}}_c\}^*} W_{\bar{\mu}}(k_\perp, k_\perp'; \ell)$$
$$\times \bar{\mathcal{O}}_{\bar{\mu}}^*(\tilde{\mathbf{k}})\mathcal{O}_{\bar{\mu}}(\tilde{\mathbf{k}}' - \tilde{\mathbf{Q}}_c) + \text{c.c}, \quad (10)$$

in which $\sum_{\mathbf{k}}$ is a sum in the outer momentum shell. Following (7), we have also defined $\sum_{\tilde{\mathbf{k}}} O_\mu(\tilde{\mathbf{k}} - \tilde{\mathbf{Q}}) = O_\mu(\tilde{\mathbf{Q}})$ for the Peierls fields, whereas in the Cooper channel, we have introduced the new fields

$$\mathcal{O}_{\bar{\mu}}(\tilde{\mathbf{k}} - \tilde{\mathbf{Q}}_c) =$$
$$\sqrt{\frac{T}{LN_\perp}} \sum_{\alpha,\beta} \alpha\, \psi_{-,-\alpha}(-\tilde{\mathbf{k}} + \tilde{\mathbf{Q}}_c)\sigma_{\bar{\mu}}^{\alpha\beta}\psi_{+,\beta}(\tilde{\mathbf{k}}) \quad (11)$$

for singlet ($\bar{\mu} = 0$; SS) and triplet ($\bar{\mu} \neq 0$; TS) pairings, where $\tilde{\mathbf{Q}}_C = (q_C, q_{\perp C}, \omega_{mC})$ corresponds to the momentum and frequency of the Cooper pair. For the fields to be integrated out in the contractions (10), the static Peierls and Cooper external variables have been set to $\tilde{\mathbf{Q}}_0 = (2k_F^0, q_\perp, 0)$ and $\tilde{\mathbf{Q}}_C = 0$ respectively.

The contraction in the Cooper channel yields the combinations of couplings

$$W_{\bar{\mu}=0} = -\frac{1}{2}J_0 + \frac{3}{2}J_{\mu\neq0}$$
$$W_{\bar{\mu}\neq0} = \frac{1}{2}J_0 + \frac{1}{2}J_{\mu\neq0} \quad (12)$$

for SS and TS Cooper pairings. The explicit evaluation of $\frac{1}{2}\langle(S_{I,2}^*)^2\rangle_{o.s}$, is given in the Appendix A. In the case of the Cooper contraction, one can invert the relations (A.4) to re-express $\frac{1}{2}\langle(S_{I,2}^C)^2\rangle_{o.s}$ in terms of pair fields of the
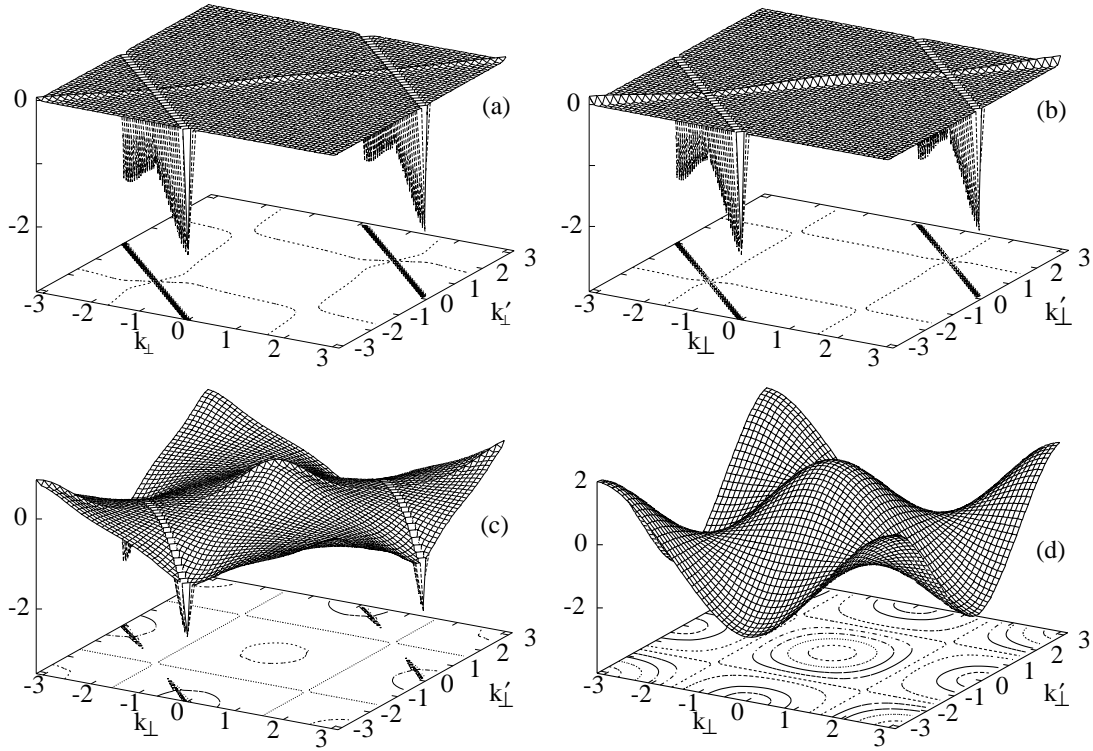
Fig. 1. Variation of the SDW coupling $J_{\mu \neq 0}(k_\perp, k'_\perp; \ell)$ in the transverse wave vector $(k_\perp, k'_\perp)$ plane close to an instability $(\ell \to \ell_{\mathrm{SDW,c}})$. (a): $t^*_{\perp 2} = 0$; (b): below but close to $t^{*c}_{\perp 2} = 6.25$ K; (c): crossover region; (d): above the crossover. The vertical scale is arbitrary.

Peierls channel. Together with $\frac{1}{2}\langle(S^P_{\mathrm{I},2})^2\rangle_{\mathrm{o.s}}$ this yields the one-loop flow equations

$$\frac{\mathrm{d}}{\mathrm{d}\ell} J_\mu(q_\perp - k_\perp, k_\perp; \ell) = \frac{1}{N_\perp} \sum_{\bar{\mu}, k'_\perp} c_{\mu, \bar{\mu}} \big[W_{\bar{\mu}}(q_\perp - k_\perp, k'_\perp; \ell)$$

$$\times W_{\bar{\mu}}(k'_\perp, k_\perp; \ell) \big] I_{\mathrm{C}}(\ell)$$

$$- J_\mu(q_\perp - k_\perp, k_\perp; \ell) \frac{1}{N_\perp} \sum_{k'_\perp} \big[J_\mu(q_\perp - k'_\perp, k'_\perp; \ell)$$

$$\times I_{\mathrm{P}}(q_\perp, k'_\perp; \ell) \big], \quad (13)$$

where the first term comes from the Cooper contraction with the constants $c_{0,0} = -1/2$, $c_{0,\bar{\mu} \neq 0} = 1/2$ and $c_{\mu \neq 0, 0} = 1/2$, $c_{\mu \neq 0, \bar{\mu} \neq 0} = 1/6$ and the thermal transient $I_{\mathrm{C}}(\ell) = \tanh[\beta E_x(\ell)/4]$. As for the Peierls contraction in the second term, a kernel $I_{\mathrm{P}}(q_\perp, k_\perp; \ell)$ follows from the evaluation of the Peierls loop which is given in Appendix A. Reverting to the initial form of the action at ℓ_x given in (4), we see that the interference between both channels does not conserve the dependence on a single transverse Peierls variable $q_\perp$ for J_μ; the scattering amplitudes now depend on both ingoing $[\pm \sim k_{\mathrm{F}}(k_\perp), k_\perp]$ and outgoing $[\mp \sim k_{\mathrm{F}}(k_\perp - q_\perp), k_\perp - q_\perp]$ momentum (note that J_μ in (10) is symmetric with respect to the interchange $k_\perp \leftrightarrow k'_\perp$). The extra $k_\perp$ dependence leads to non-uniform electron-hole pairing, which gives valuable information about the strength of the scattering matrix el-

ement and in turn the formation of the order parameter along the Fermi surface.

The information concerning density-wave or superconducting instabilities of the normal state is obtained from the singularities of the flow equations. Although 2D systems cannot sustain these forms of long-range order at finite temperature (or finite ℓ), the temperature $T_i = E(\ell_i)/2$ at which the singularity occurs is nevertheless indicative of the temperature range of true long-range ordering if a finite coupling in the third direction is added. Tackling first the possibility of a SDW instability in the absence of nesting deviations $(t^*_{\perp 2} = 0)$ and when repulsive interactions $g^*_{i=1,2}$, $j_\perp$ prevail at E_x, the SDW coupling $J_{\mu \neq 0}(q_\perp - k_\perp, k_\perp; \ell)$ is found to be the most singular as a function of ℓ. By way of illustration, if we take $g_1 = 0.71$, $g_2 = 0.80$ and $t_\perp = 160$ K at $E_{\mathrm{F}} = 3600$ K, the 1D two-loop RG results yield [25], $g^*_1 = 0.17$, $g^*_2 = 0.54$, and $j_{\perp \mu \neq 0(0)} = 0.33(0.024)$ as boundary conditions at $E_x = t^*_\perp = 120$ K. Thus feeding (13) with the latter initial conditions, the solution of the flow equation does predict a singularity at ℓ_{SDW} corresponding to a critical temperature $T_{\mathrm{SDW}} = E_x(\ell_{\mathrm{SDW}})/2 \approx 8.5$ K, which falls in the range of experimental T_{SDW} in $(\mathrm{TM})_2\mathrm{X}$ when metallic conditions prevail and nesting deviations $(t_{\perp 2})$ are small [19]. The singularity occurs along the lines $k'_\perp = \pm \pi - k_\perp$ (Fig. 1a) and is associated with the SDW modulation vector $\mathbf{Q}_{\mathrm{P}} = (2k^0_{\mathrm{F}}, q_\perp = \pi)$ which is the best nesting vector of the model. On closer examination, Figure 1a shows that the scattering amplitude is not uniform, especially in
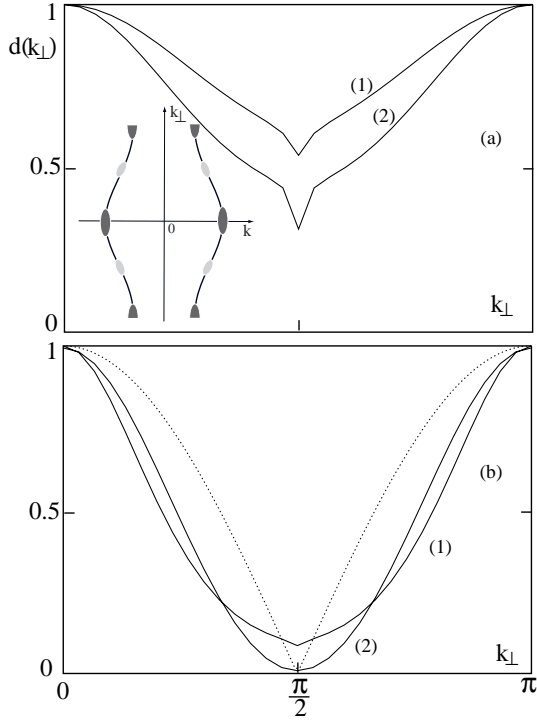
Fig. 2. Variation of the SDW normalized scattering amplitude $d(k_\perp) \equiv J_{\mu \neq 0}(\pi - k_\perp, k_\perp)/J_{\mu \neq 0}^{\max}$ close to $\ell_{\mathrm{SDW,c}}$ or the gap ($\Delta_{\mu \neq 0} \propto d(k_\perp)$) below T_{SDW} along the Fermi surface $k_{\mathrm{F}}(k_\perp)$ parametrized by $k_\perp$. (a): below the threshold for $t_{\perp 2}^* = 0$ (1), and $t_{\perp 2}^*$ close to $t_{\perp 2}^{*c}$ (2); (b): above the threshold for $t_{\perp 2}^*$ close to $t_{\perp 2}^{*c}$ in the crossover region (1) and $t_{\perp 2}^*$ above the crossover domain (2). The dashed curve corresponds to the variation of the interchain singlet gap along the Fermi surface $|\Delta(k_\perp)|/\Delta_0 = |\cos k_\perp|$. The inset of (a) shows the location of cold (light) and hot (dark) spots on the Fermi surface.

regions centered at $k_\perp = \pm \pi/2$ (resp. $k_\perp = 0, \pm\pi$), which can be seen as 'cold spots' (resp. hot spots) where a decrease of $\sim 50\%$ in the scattering intensity is found. This variation denoted $d(k_\perp)$ in Figure 2 reflects in turn the one of the SDW order parameter along the Fermi surface [26]. Therefore the interference with the Cooper channel modifies significantly the variation of the SDW gap along the Fermi surface even though nesting deviations are absent. As we will see below, these cold regions actually coincide with the nodes of an interchain superconducting gap at sufficiently large $t_{\perp 2}^*$.

Now if we try to mimic the influence of pressure, its effect can be parametrized through the growth of $t_{\perp 2}^*$. Thus by taking $\mathrm{d}E_{\mathrm{F}}(v_{\mathrm{F}})/\mathrm{d}t_{\perp 2}^* \approx 90$, the RG procedure in the 1D regime [25] gives $\mathrm{d}g_{1(2)}^*/\mathrm{d}t_{\perp 2}^* \approx -2.5\%(-4\%)/\mathrm{K}$, $\mathrm{d}j_{\perp \mu \neq 0(0)}/\mathrm{d}t_{\perp 2}^* \approx -4\%(-8\%)/\mathrm{K}$ and $\mathrm{d}E_x/\mathrm{d}t_{\perp 2}^* \approx 5$. These variations lead to a monotonic decrease of T_{SDW} at small $t_{\perp 2}^*$ and ultimately initiate a rapid drop of T_{SDW} (Fig. 3). Along this drop, the electron system, albeit still unstable to the formation SDW order, develops a scattering amplitude and in turn an order parameter that is highly non uniform on the Fermi surface. 'Hot' (resp. 'cold') spots close to $(\sim \pm k_{\mathrm{F}}(k_\perp), k_\perp = 0, \pm\pi)$ [resp.
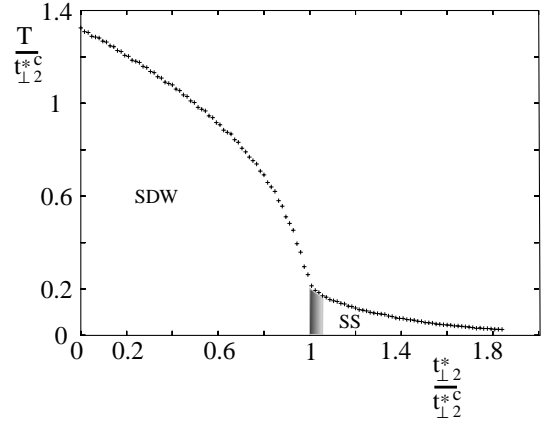
Fig. 3. Variation of the critical temperature as a function of the amplitude of nesting deviations $t_{\perp 2}^*$. The shaded area corresponds to the crossover region where reentrant superconductivity can occur.

($\sim \pm k_{\mathrm{F}}(k_\perp), k_\perp = \pm \pi/2$)] are really taking shape and their locations on the Fermi surface are kept fixed by the interaction with Cooper pairing as $t_{\perp 2}^*$ varies (Figs. 1, 2). This contrasts with the results of mean-field theory of the SDW state for which only nesting deviations are involved and lead to a qualitatively different variation of the gap [27]. As we will see below, a non uniform gap leads to an important reduction of condensation energy for the SDW state.

As $t_{\perp 2}^*$ is further increased, the critical line in Figure 3 develops an inflexion point at $t_{\perp 2}^{*c}$ ($t_{\perp 2}^{*c} \approx 6.25$ K using the above figures) above which the scattering amplitude becomes warped by a singular modulation in the $k_\perp, k_\perp'$ plane at ℓ_c (Fig. 1c). This signals an instability at $T_c = E_x(\ell_c)/2$, which involves an additional channel connected with superconductivity. In order to see what type of superconducting pairing scales to strong coupling, it is natural to make a Fourier decomposition of J_μ. Given the relation for the scattering amplitude in S, that is

$$-\sum_\mu \sum_{\{\tilde{\mathbf{k}}, \tilde{\mathbf{k}}', \tilde{\mathbf{Q}}\}^*} J_\mu(q_\perp - k_\perp, k_\perp'; \ell) O_\mu^*(\tilde{\mathbf{k}} + \tilde{\mathbf{Q}}) \, O_\mu(\tilde{\mathbf{k}}' - \tilde{\mathbf{Q}})$$

$$= \sum_{\bar{\mu}} \sum_{\{\tilde{\mathbf{k}}, \tilde{\mathbf{k}}', \tilde{\mathbf{Q}}_c\}^*} W_{\bar{\mu}}(k_\perp, k_\perp'; \ell) \, \mathcal{O}_{\bar{\mu}}^*(\tilde{\mathbf{k}} + \tilde{\mathbf{Q}}_c) \, \mathcal{O}_{\bar{\mu}}(\tilde{\mathbf{k}}' - \tilde{\mathbf{Q}}_c)$$

(14)

and the property $W_{\bar{\mu}}(k_\perp, k_\perp'; \ell) = W_{\bar{\mu}}(-k_\perp, -k_\perp'; \ell)$, one can write

$$W_{\bar{\mu}}(k_\perp, k_\perp'; \ell) = a_{\bar{\mu}}^0(\ell)$$
$$+ \sum_{m,n>0}^\infty \left[a_{\bar{\mu}}^{m,n}(\ell) \cos(mk_\perp) \cos(nk_\perp') \right.$$
$$\left. + b_{\bar{\mu}}^{m,n}(\ell) \sin(mk_\perp) \sin(nk_\perp') \right], \quad (15)$$

which allows one to express the interaction in the Cooper channel as a sum of potential with separate variables with Fourier coefficients $a_{\bar{\mu}}^{m,n}(\ell)$ and $b_{\bar{\mu}}^{m,n}(\ell)$ that are scale dependent (here the coefficients $a^{m,n}$ and $b^{m,n}$ with $m \neq n$

are essentially zero). In this way, to each Fourier amplitude corresponds an *interchain* superconducting coupling of different orbital symmetry in the SS ($\bar{\mu} = 0$) and TS ($\bar{\mu} \neq 0$) channels. As is obvious from the parity of the modulation in Figures 1c–d, the positive coefficient $a_{\bar{\mu}=0}^{1,1}(\ell)$ of the first harmonic dominates and is singular at ℓ_c; it corresponds to an instability for *singlet* ($\bar{\mu} = 0$) pairing between nearest-neighbor chains having a symmetric orbital part and a spin part that is antisymmetric. From (12), a smaller contribution of the same Fourier coefficient also applies to triplet superconductivity ($\bar{\mu} \neq 0$), but this pairing is not globally antisymmetric and remains inactive for both short-range and long-range orders. Actually, our results show that the first positive triplet pairing coefficient satisfying symmetry requirements is rather contained in the much smaller Fourier coefficient $b_{\bar{\mu} \neq 0}^{2,2}(\ell)$ having odd orbital parity for pairing between second nearest-neighbor chains.

One can then define a finite $t_{\perp 2}^*$ interval above $t_{\perp 2}^{*c}$ in which both $\mathrm{SS}(a_{\bar{\mu}=0}^{1,1})$ and $\mathrm{SDW}(J_{\mu \neq 0})$ pairings scale to strong coupling. This region is delimited by a shaded area in Figure 3 and can be equated with the SDW-SS crossover region. Although a one-loop weak coupling approach does not allow one to make definite conclusions about the actual structure of the phase diagram in the crossover domain, from the variation of the strength of electron-hole pairing $J_{\mu \neq 0}$ (or the SDW gap) across the Fermi surface (Fig. 2b), it is possible at a more qualitative level to infer that superconductivity will be the most stable state at low temperature in that region of the phase diagram (*cf.* Sect. 3.3).

The regular but rapid variation under pressure of $T_c(t_{\perp 2}^*)$ above the crossover in Figure 3 can be obviously understood as the reduction of the density-wave correlations that feed the Cooper channel.

3.2 Response functions

The temperature dependence of the amplitude of correlations leading to the instabilities of the phase diagram can be obtained from the calculation of response functions in both Peierls and Cooper channels. To do so in the RG framework, we follow the work of reference [25] and couple the electrons to a set of source fields at E_x

$$S_h[\psi^*, \psi] = \sum_{\mu} z_{\mu} \left[O_{\mu}^*(\mathbf{Q}_\mathrm{P}) h_{\mu}(\mathbf{Q}_\mathrm{P}) + \mathrm{c.c} \right]$$
$$+ \sum_{\bar{\mu}, \{\tilde{\mathbf{k}}\}^*} z_{\bar{\mu}}^{(n)} \left[\mathcal{O}_{\bar{\mu}}^*(\tilde{\mathbf{k}}) h_{\bar{\mu}}^{(n)}(k_\perp) + \mathrm{c.c} \right], \quad (16)$$

where the source fields h_μ are taken independent of the frequency for the static response at $\mathbf{Q}_\mathrm{P} = (2k_\mathrm{F}^0, \pi)$ in the Peierls channel; whereas in the Cooper channel we are interested in the nth harmonic of the static interstack pairing response at $\tilde{\mathbf{Q}}_\mathrm{C} = 0$ with $h_0^{(n)}(k_\perp) = h_0^{(n)} \cos(nk_\perp)$ for SS and $h_{\bar{\mu} \neq 0}^{(n)}(k_\perp) = h_{\bar{\mu} \neq 0}^{(n)} \sin(nk_\perp)$ for TS. Here the

$z_{\mu(\bar{\mu})}^{(n)}$ are the corresponding vertex corrections, which for simplicity are put equal to unity at E_x [28].

Performing successive partial traces according to (9), the one-loop corrections yield

$$S_h[\psi^*, \psi]_\ell = \sum_{\mu} z_{\mu}(\ell) \left[O_{\mu}^*(\mathbf{Q}_\mathrm{P}) h_{\mu}(\mathbf{Q}_\mathrm{P}) + \mathrm{c.c} \right]$$
$$+ \sum_{\bar{\mu}, \{\tilde{\mathbf{k}}\}^*} z_{\bar{\mu}}^{(n)}(\ell) \left[\mathcal{O}_{\bar{\mu}}^*(\tilde{\mathbf{k}}) h_{\bar{\mu}}^{(n)}(k_\perp) + \mathrm{c.c} \right]$$
$$+ \sum_{\mu} \chi_{\mu}(\ell) h_{\mu}^*(\mathbf{Q}_\mathrm{P}) h_{\mu}(\mathbf{Q}_\mathrm{P})$$
$$+ \sum_{\bar{\mu}, k_\perp} \chi_{\bar{\mu}}^{(n)}(\ell) h_{\bar{\mu}}^{(n)*}(k_\perp) h_{\bar{\mu}}^{(n)}(k_\perp), \quad (17)$$

where the pair vertex corrections are obtained from the contractions $\langle S_{\mathrm{I},2} S_{\mathrm{h},2} \rangle_{\mathrm{o.s}}$ which involved electron-hole and electron-electron loops whose evaluation is similar to the one given in Appendix A. The pair vertex parts are then governed by the flow equations

$$\frac{\mathrm{d}}{\mathrm{d}\ell} \ln z_{\mu}(\ell) = -\frac{1}{N_\perp} \sum_{k_\perp} \left[J_{\mu}(\pi - k_\perp, k_\perp; \ell) \right.$$
$$\left. \times I_\mathrm{P}(\pi, k_\perp; \ell) \right] \quad (18)$$

in the Peierls channel and

$$\frac{\mathrm{d}}{\mathrm{d}\ell} \ln z_{\bar{\mu}=0}^{(n)}(\ell) = \frac{1}{2} a_{\bar{\mu}=0}^{n,n}(\ell) I_\mathrm{C}(\ell) \quad (19)$$

$$\frac{\mathrm{d}}{\mathrm{d}\ell} \ln z_{\bar{\mu} \neq 0}^{(n)}(\ell) = \frac{1}{2} b_{\bar{\mu} \neq 0}^{n,n}(\ell) I_\mathrm{C}(\ell), \quad (20)$$

in the Cooper channel.

The last two terms in (17) come from the contraction $\frac{1}{2} \langle S_{\mathrm{h},2}^2 \rangle_{\mathrm{o.s}}$, which generates expressions that are quadratic in the source fields and whose coefficients

$$\chi_{\mu(\bar{\mu})}^{(n)}(\ell) = (\pi v_\mathrm{F})^{-1} \int_0^\ell [z_{\mu(\bar{\mu})}^{(n)}(\ell')]^2 \, \mathrm{d}\ell' \quad (21)$$

correspond to the static response function (defined as positive). From the integration of the flow equations for the pair vertex parts (18–20), the temperature dependence of SDW and SC pairing responses are calculated with the set of coupling parameters used in Figure 3. Below $t_{\perp 2}^{*c}$, the SDW response dominates for all temperatures and becomes singular at T_SDW (Figs. 4a, b). In the crossover region, however, both SDW and SS become large but it is only very close to T_c that the amplitude of SS response catches up with the SDW one (Fig. 4c). Finally above the crossover (Fig. 4d), the SS correlations diverge at T_c whereas SDW correlations, albeit still enhanced, show no sign of singular behavior. In Figures 4c, d, we verify that the amplitude of interstack $n = 2$ triplet superconducting response $\chi_\mathrm{TS}^{(2)}(T)$ is scarcely enhanced so it essentially merges with the free or non interacting (logarithmic) limit $\chi_\mathrm{Free}(T)$ over the whole temperature range.
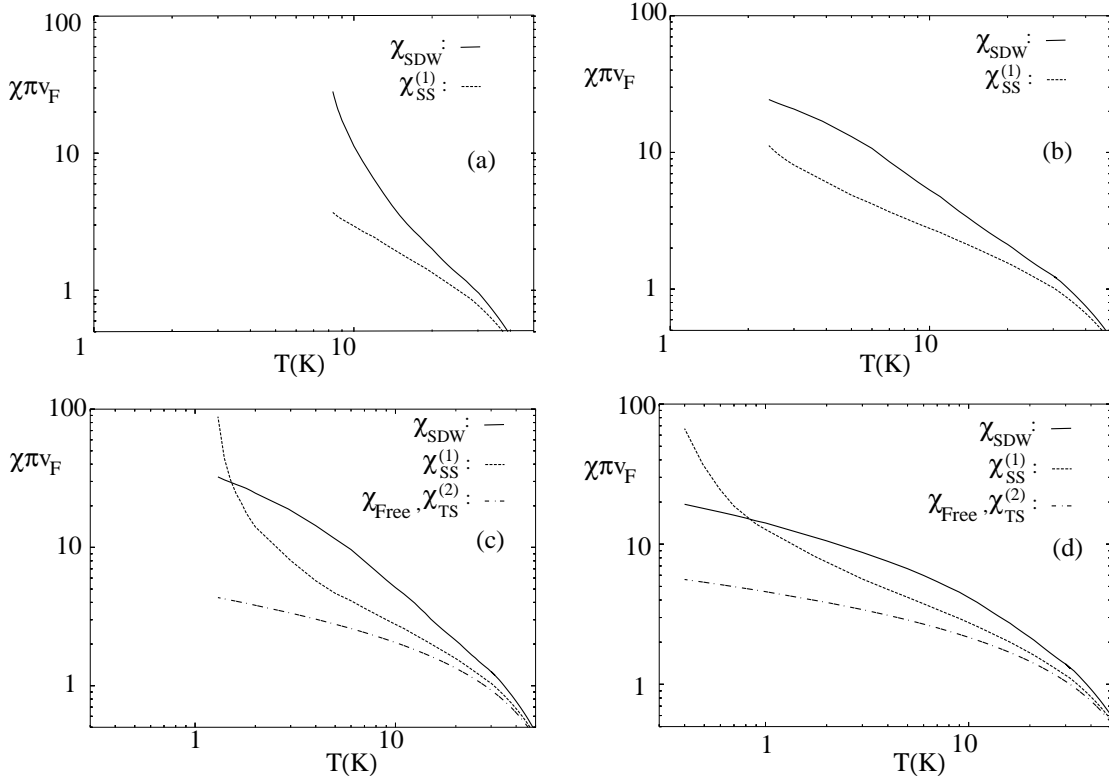
Fig. 4. Response functions at $t_{\perp 2}^* = 0$ (a), close to but below (b) and above the threshold (c) $t_{\perp 2}^{*c}$, and well above $t_{\perp 2}^{*c}$ (d).

3.3 On the possibility of reentrant superconductivity

Before closing this section, we would like to examine on a qualitative basis the consequences of non uniform pairing on the relative stability of the SDW and SS order parameters in the crossover region. In the light of the above results, the profile of the SDW scattering amplitude $J_\mu(k_\perp - q_\perp, k_\perp; \ell)$, albeit singular on the lines $q_\perp = \pm\pi$ for all $k_\perp$ as $\ell \to \ell_{\text{SDW,c}}$ (Figs. 1a–c, 2, 4a–c), reflects the variation $d(k_\perp)$ of the order parameter and in turn the one of the SDW gap $\Delta_{\mu\neq 0}(k_\perp)$ along the Fermi surface within the ordered phase. Therefore if the SDW transition occurs first, the reduction of the gap in cold regions will lower the SDW condensation energy with respect to the case where a uniform gap would be created. This reduction along with the one of T_{SDW} (Fig. 3) continues up to the crossover region where the condensation energy becomes comparable and ultimately weaker than the one of a superconducting ordered state having a lower critical temperature but a singlet gap $\Delta(k_\perp) = |\Delta_0|\cos k_\perp$ that would be more developed along the Fermi surface (Fig. 2b). This crossing of condensation energy will then signal a first-order transition from SDW to the SS state − a possibility known as reentrant superconductivity as pointed out by Yamaji in the framework of a phenomenological mean-field theory of the competition between SDW and s-wave states in the Bechgaard salts [29].

A quantitative analysis of reentrance in the present context would require a microscopic derivation of the tem-

perature dependent Landau free energy at $T < T_{\text{SDW}}$, which includes interference effects between the density-wave and Cooper channels, a derivation that is beyond the scope of the present paper. More qualitatively, however, it is possible to estimate the extent of the reentrance on the $t_{\perp 2}^*$ scale by making few assumptions on the form taken by condensation energy in the zero temperature limit. Thus if the drop in energy (here expressed per chain and per unit of length) with respect to the normal phase can be expanded in powers of the gap, one can write in lowest order

$$\delta E_i[\Delta_i] \simeq -\frac{1}{2}(\pi v_{\text{F}})^{-1} C_i \frac{1}{N_\perp} \sum_{k_\perp} \Delta_i^2(k_\perp) + \dots, \quad (22)$$

for i =SDW and SS, where C_i is a constant (within the mean-field (BCS) theory, $C_i = 1$, and δE_i is purely quadratic [30]). Taking $\Delta_{\text{SDW}}(k_\perp) = |\Delta_{\mu\neq 0}| \, d(k_\perp)$ and $\Delta_{\text{SS}}(k_\perp) = |\Delta_0| \cos k_\perp$ for the SDW and a SS gaps respectively and assuming a BCS-like correspondence $|\Delta_i| \sim T_{\text{c,i}}$ between the maximum amplitude of the gap at zero temperature and the critical temperature, the ratio of condensation energies will take the approximate form

$$\frac{\delta E_{\text{SDW}}}{\delta E_{\text{SS}}} \approx \frac{T_{\text{SDW}}^2}{T_c^2} 2 N_\perp^{-1} \sum_{k_\perp} d^2(k_\perp). \quad (23)$$

Thus by extracting $d(k_\perp)$ from the normalized scattering amplitude along $k'_\perp = \pm\pi - k_\perp$ (Fig. 2b), the ratio of condensation energies becomes invariably smaller than unity

for T_c not too far below T_{SDW} in the crossover region. This indicates that whenever SDW is first stabilized in that part of phase diagram, the conditions are favorable for reentrant superconductivity. The corresponding SDW-SS equilibrium curve should join the critical line with a positive slope.

4 Concluding remarks

In the light of previous results interesting conclusions can be drawn. Concerning first the applications to real materials like the Bechgaard salts and their sulfur analogs, the present approach may serve as a microscopic basis towards a synthesis of itinerant antiferromagnetism and unconventional superconductivity in these compounds. This would include the description of systems like the spin-Peierls Fabre salt $(TMTTF)_2PF_6$ for which a crossover from itinerant antiferromagnetism to superconductivity has been found under very high pressure [20,31,32].

The interplay between SDW and SS correlations has various impacts which may cast new light on both types of ordering. Starting with the normal phase, the calculation of the response functions shows that both types of correlations can be enhanced in the same temperature domain, indicating that the different ordering factors interfere constructively − this is particularly manifest within the narrow confines of reentrant superconductivity in the crossover domain. Another impact concerns the description of the SDW state itself, which shows qualitative difference with respect to mean-field prediction as a result of interference with superconductivity. All this goes to show that nesting conditions do not govern alone the characterization of the SDW state, but that Cooper pair correlations have a determining influence leaving their stamp on electron-hole pairing or the SDW gap along the Fermi surface. The impact of interference on the properties of normal state in the vicinity of a SDW ordering is also of interest. It indeed provides a microscopic basis as to the origin and the location of cold and hot spots on the Fermi surface which are suspected to be important in explaining anomalous magnetotransport effects close to $t^{*c}_{\perp 2}$ [33,34].

The physical picture of interfering channels in the emergence of superconductivity naturally connects to the physics of the field-induced SDW states in which geometrical properties (nesting) of the Fermi surface play such an important role [27,35,36]. In this matter, it would be worth examining the weakening of the interference when a magnetic field is turned on close to the crossover on the SS side, namely where FISDW states are found [37]. The presence of a field (oriented properly) will weaken both the infrared singularity of the Cooper channel and nesting deviations, which should tip the balance in favour of a single channel or mean-field description [35,36]. However, it is possible that some traces of interference are still present and may affect to some extent the profile of the gap and hence the properties of the FISDW state.

The present theoretical weak coupling calculation of the critical temperatures cannot pretend to be quantitative, given the reduction of variables in obtaining the flow equations, especially those related to dynamical (retardation) effects which are likely to become relevant within the crossover region when both SDW and SS pairings scale to strong coupling. However we think that our approach embodies the essential ingredients of the competition between SDW and SC states in these materials.

Appendix A: One-loop contractions

A.1 Cooper channel

From the last term of the outer shell decomposition in (10), the contraction in the Cooper channel evaluated at $\tilde{\mathbf{Q}}_c = 0$ reads

$$\frac{1}{2} \ \langle (S^C_{I,2})^2 \rangle_{o.s} = (\pi v_F)^2 \sum_{\bar{\mu}_1,\bar{\mu}_2} \sum_{\{\tilde{\mathbf{k}},\tilde{\mathbf{k}}'\tilde{\mathbf{Q}}_C\}^*} \sum_{\{\tilde{\mathbf{k}}_1,\tilde{\mathbf{k}}_2\}}$$
$$\times \ \langle W_{\bar{\mu}_1}(k_\perp, k_{\perp,1}; \ell) \bar{\mathcal{O}}^*_{\bar{\mu}_1}(\tilde{\mathbf{k}}_1) \bar{\mathcal{O}}_{\bar{\mu}_2}(\tilde{\mathbf{k}}_2) W_{\bar{\mu}_2}(k_{\perp,2}, k'_\perp; \ell) \rangle$$
$$\times \ \mathcal{O}^*_{\bar{\mu}_2}(\tilde{\mathbf{k}} + \tilde{\mathbf{Q}}_C) \mathcal{O}_{\bar{\mu}_1}(\tilde{\mathbf{k}}' - \tilde{\mathbf{Q}}_C) \, \delta_{\bar{\mu}_1,\bar{\mu}_2} \delta_{\tilde{\mathbf{k}}_1,\tilde{\mathbf{k}}_2}, \quad (A.1)$$

where the outer shell average is given by

$$\sum_{\tilde{\mathbf{k}}_1} \langle W_{\bar{\mu}}(k_\perp, k_{\perp 1}; \ell) \bar{\mathcal{O}}^*_{\bar{\mu}}(\tilde{\mathbf{k}}_1) \bar{\mathcal{O}}_{\bar{\mu}}(\tilde{\mathbf{k}}_1) W_{\bar{\mu}}(k_{\perp 1}, k'_\perp; \ell) \rangle$$

$$= 2 \frac{T}{LN_\perp} \sum_{\omega_n} \sum_{\mathbf{k}_1} \left[W_{\bar{\mu}}(k_\perp, k_{\perp 1}; \ell) G^0_+(\mathbf{k}_1, \omega_n) \right.$$
$$\left. \times G^0_-(-\mathbf{k}_1, -\omega_n) W_{\bar{\mu}}(k_{\perp 1}, k'_\perp; \ell) \right]$$
$$= (2\pi v_F)^{-1} \frac{1}{N_\perp} \sum_{k_{\perp 1}} W_{\bar{\mu}}(k_\perp, k_{\perp 1}; \ell) W_{\bar{\mu}}(k_{\perp 1}, k'_\perp; \ell)$$
$$\times \int_{o.s} \frac{\tanh \frac{\beta}{2} E_+}{E_+} dE_+, \quad (A.2)$$

where the last line follows from the frequency sum and the use of the relation

$$\frac{1}{2\pi} \iint \frac{dS dE_+}{|\nabla E_+|} \ldots = \frac{1}{N_\perp v_F} \sum_{k_{\perp 1}} \int dE_+ \ldots$$

for the curve integral over constant energy shell. The integral in the outer energy shell is made over the intervals $[-E_x(\ell)/2, -E_x(\ell+d\ell)/2]$ and $[E_x(\ell+d\ell)/2, E_x(\ell)/2]$, and

yields the result for the Cooper contraction

$$\frac{1}{2}\langle (S_{I,2}^{C})^2\rangle_{o.s} = \pi v_F \sum_{\{\tilde{\mathbf{k}},\tilde{\mathbf{k}}'\}^*} \frac{d\ell}{N_\perp} \sum_{k_{\perp 1}} \big[W_{\bar{\mu}}(k_\perp, k_{\perp 1}; \ell)$$
$$\times W_{\bar{\mu}}(k_{\perp 1}, k'_\perp; \ell) \, I_C(\ell) \, \mathcal{O}_{\bar{\mu}}^*(\tilde{\mathbf{k}} + \tilde{\mathbf{Q}}_C)\mathcal{O}_{\bar{\mu}}(\tilde{\mathbf{k}}' - \tilde{\mathbf{Q}}_C),$$
$$(A.3)$$

where $I_C(\ell) = \tanh[\beta E_x(\ell)/4]$. Using the relations

$$\sum_{\{\tilde{\mathbf{k}},\tilde{\mathbf{k}}',\tilde{\mathbf{Q}}\}} O_0^*(\tilde{\mathbf{k}} + \tilde{\mathbf{Q}})O_0(\tilde{\mathbf{k}}' - \tilde{\mathbf{Q}}) =$$
$$\sum_{\{\tilde{\mathbf{k}},\tilde{\mathbf{k}}',\tilde{\mathbf{Q}}_C\}} \big\{ \frac{1}{2}\mathcal{O}_{\bar{\mu}=0}^*(\tilde{\mathbf{k}} + \tilde{\mathbf{Q}}_C)\mathcal{O}_{\bar{\mu}=0}(\tilde{\mathbf{k}}' - \tilde{\mathbf{Q}}_C)$$
$$-\frac{1}{2}\sum_{\bar{\mu}\neq 0} \mathcal{O}_{\bar{\mu}}^*(\tilde{\mathbf{k}} + \tilde{\mathbf{Q}}_C)\mathcal{O}_{\bar{\mu}}(\tilde{\mathbf{k}}' - \tilde{\mathbf{Q}}_C) \big\}$$
$$\sum_{\{\tilde{\mathbf{k}},\tilde{\mathbf{k}}',\tilde{\mathbf{Q}}\}}\sum_{\mu\neq 0} O_\mu^*(\tilde{\mathbf{k}} + \tilde{\mathbf{Q}})O_\mu(\tilde{\mathbf{k}}' - \tilde{\mathbf{Q}}) =$$
$$\sum_{\{\tilde{\mathbf{k}},\tilde{\mathbf{k}}',\tilde{\mathbf{Q}}_c\}} \big\{ -\frac{3}{2}\mathcal{O}_{\bar{\mu}=0}^*(\tilde{\mathbf{k}} + \tilde{\mathbf{Q}}_C)\mathcal{O}_{\bar{\mu}=0}(\tilde{\mathbf{k}}' - \tilde{\mathbf{Q}}_C)$$
$$-\frac{1}{2}\sum_{\bar{\mu}\neq 0}\mathcal{O}_{\bar{\mu}}^*(\tilde{\mathbf{k}} + \tilde{\mathbf{Q}}_C)\mathcal{O}_{\bar{\mu}}(\tilde{\mathbf{k}}' - \tilde{\mathbf{Q}}_C)\big\}, \quad (A.4)$$

this result can be rewritten in terms of products of Peierls fields contributing to the first term of the flow equation for J_μ (Eq. (13)).

A.2 Peierls channel

From the first two terms of (10), the contractions in the Peierls channel are given by

$$\frac{1}{2}\langle (S_{I,2}^{P})^2\rangle_{o.s} = (\pi v_F)^2 \sum_{\mu_1,\mu_2} \sum_{\{\tilde{\mathbf{k}},\tilde{\mathbf{k}}',\tilde{\mathbf{Q}}\}^*} \sum_{\{\tilde{\mathbf{k}}_1,\tilde{\mathbf{k}}_2\}}$$
$$\times \big[\langle J_{\mu_1}(q_\perp - k_{\perp 1}, k_{\perp 1}; \ell)\bar{O}_{\mu_1}^*(\tilde{\mathbf{k}}_1 + \tilde{\mathbf{Q}}_0)\bar{O}_{\mu_2}(\tilde{\mathbf{k}}_2 - \tilde{\mathbf{Q}}_0)$$
$$\times J_{\mu_2}(q_\perp - k'_\perp, k'_\perp; \ell)O_{\mu_2}^*(\tilde{\mathbf{k}} + \tilde{\mathbf{Q}})O_{\mu_1}(\tilde{\mathbf{k}}' - \tilde{\mathbf{Q}})$$
$$\times \delta_{\mu_1,\mu_2}\delta_{\tilde{\mathbf{k}}_1+\tilde{\mathbf{Q}}_0,\tilde{\mathbf{k}}_2}\big], \quad (A.5)$$

in which we define

$$F(q_\perp) = \sum_{\tilde{\mathbf{k}}_1}\langle J_\mu(q_\perp - k_{\perp 1}, k_{\perp 1}; \ell')\bar{O}_\mu^*(\tilde{\mathbf{k}}_1 + \tilde{\mathbf{Q}}_0)\bar{O}_\mu(\tilde{\mathbf{k}}_1)\rangle$$
$$= -2\frac{T}{LN_\perp}\sum_{\omega_n}\sum_{\mathbf{k}_1}\big[J_\mu(q_\perp - k_{\perp 1}, k_{\perp 1}; \ell)$$
$$\times G_+^0(\mathbf{k}_1 + \tilde{\mathbf{Q}}_0, \omega_n)G_-^0(\mathbf{k}_1, \omega_n). \quad (A.6)$$

As a function of $q_\perp$, the electron and hole of the Peierls loop cannot be put simultaneously in the outer energy shell for all values of $k_{\perp 1}$ in the Brillouin zone. Parts of the $k_{\perp 1}$ summation would then refer to J_μ obtained at previous values of ℓ. However, this variation of J_μ with ℓ within the $k_{\perp 1}$ interval will be neglected consistently with

the absence of dependence on the longitudinal momentum for the couplings. After a frequency sum, one then finds

$$F(q_\perp) = (2\pi v_F)^{-1}\frac{1}{N_\perp}\sum_{k_{\perp 1}} J_\mu(q_\perp - k_{\perp 1}, k_{\perp 1}; \ell)$$
$$\times \int_{o.s} \frac{\tanh\frac{\beta}{2}[E_- + A(k_{\perp 1}, q_\perp)] + \tanh\frac{\beta}{2}E_-}{2E_- + A(k_{\perp 1}, q_\perp)}\, dE_-,$$
$$(A.7)$$

where

$$A(k_{\perp 1}, q_\perp) = 2t_\perp^*[\cos k_{\perp 1} + \cos(k_{\perp 1} + q_\perp)]$$
$$+ 2t_{\perp 2}^*[\cos 2k_{\perp 1} + \cos(2k_{\perp 1} + 2q_\perp)]. \quad (A.8)$$

Integrating in the outer energy shell yields

$$\frac{1}{2}\langle (S_{I,2}^{P})^2\rangle_{o.s} = (\pi v_F)\sum_\mu \sum_{\{\tilde{\mathbf{k}},\tilde{\mathbf{k}}',\tilde{\mathbf{Q}}\}^*} \frac{d\ell}{N_\perp}\sum_{k_{\perp 1}}$$
$$\times \big[I_P(q_\perp, k_{\perp 1}, \ell)J_\mu(q_\perp - k_{\perp 1}, k_{\perp 1}; \ell)$$
$$\times J_\mu(q_\perp - k'_\perp, k'_\perp; \ell)\big]$$
$$\times O_\mu^*(\tilde{\mathbf{k}} + \tilde{\mathbf{Q}})O_\mu(\tilde{\mathbf{k}}' - \tilde{\mathbf{Q}}), \quad (A.9)$$

where

$$I_P(q_\perp, k_{\perp 1}, \ell) = \frac{E_x(\ell)}{4}\sum_{p=\pm}\Big[\tanh\frac{\beta}{4}E_x(\ell)$$
$$+ \tanh\frac{\beta}{2}[E_x(\ell)/2 + pA(k_{\perp 1}, q_\perp)]\Big]/[E_x(\ell) + pA(k_{\perp 1}, q_\perp)].$$
$$(A.10)$$

References

1. D.J. Scalapino, Phys. Rep. **250**, 329 (1995).
2. P.W. Anderson, Science **235**, 1185 (1987).
3. S.-C. Zhang, Science **275**, 1089 (1997).
4. V.J. Emery, Synthetic Metals **13**, 21 (1986).
5. M.T. Béal-Monod, C. Bourbonnais, V.J. Emery, Phys. Rev. B **34**, 7716 (1986).
6. L.G. Caron, C. Bourbonnais, Physica B **143**, 453 (1986).
7. V.J. Emery, R. Bruisma, S. Barisic, Phys. Rev. Lett. **48**, 1039 (1982).
8. V.J. Emery, J. Phys. Colloq. France **44**, C3-977 (1983).
9. W. Kohn, J.M. Luttinger, Phys. Rev. Lett. **15**, 524 (1965).
10. C. Bourbonnais, L.G. Caron, Europhys. Lett. **5**, 209 (1988).
11. B. Guay, C. Bourbonnais, Synthetic Metals **103**, 2180 (1999).
12. C. Seidel, V.N. Prigodin, J. Phys. Lett. France **44**, L403 (1983).
13. K. Yamaji, J. Phys. Soc. Jpn **51**, 2787 (1982).
14. Y. Hasegawa, H. Fukuyama, J. Phys. Soc. Jpn **56**, 877 (1987).
15. H. Shimahara, J. Phys. Soc. Jpn **58**, 1735 (1989).
16. H. Kino, H. Kontani, J. Phys. Soc. Jpn **68**, 1481 (1999).

17. V.N. Prigodin, Y.A. Firsov, Sov. Phys. JETP **49**, 369 (1979).
18. For the application of the RG method in the context of isotropic 2D systems as a function of band filling, see for example D. Zanchi, H.J. Schulz, Phys. Rev. B **61**, 13 609 (2000); C. Honerkamp, M. Salmhofer, N. Furukawa, T.M. Rice Phys. Rev. B **63**, 35109 (2001); C.J. Halborth, W. Metzner, Phys. Rev. B **85**, 5164 (2000) and references there cited.
19. D. Jérome, H. Schulz, Adv. Phys. **31**, 299 (1982).
20. D. Jaccard *et al.*, J. Phys. Cond. Matt. **13**, 89 (2001).
21. For arguments in favor of triplet superconductivity in the Bechgaard salts, see for example I.J. Lee *et al.*, cond-mat/0001332.
22. J. Solyom, Adv. Phys. **28**, 201 (1979).
23. If the energy scale for electronic deconfinement is greater than the 1D Mott (insulating) gap Δ_ρ induced by umklapp scattering, the system remains metallic down to the SDW ordering temperature. In the low temperature metallic domain umklapp scattering is present but its influence for long-range order stands at a more quantitative level. It can be included in the present simplified (g_1, g_2) model through a redefinition of the g_2^* coupling at E_x (Eq. (8)). A more complete discussion of umklapp processes will be presented elsewhere.
24. T. Giamarchi, Physica B **230-232**, 975 (1997).
25. C. Bourbonnais, L.G. Caron, Int. J. Mod. Phys. B **5**, 1033 (1991).
26. Within a one-body description of the SDW state, a quasi-particle spectrum of the form $E_p^{*\pm}(\mathbf{k}) = \pm\sqrt{E_p^{*2}(\mathbf{k}) + \Delta_{\mu \neq 0}^2(k_\perp)}$, has a gap function $\Delta_{\mu \neq 0}(k_\perp)$ which is proportional to the scattering amplitude $J_{\mu \neq 0}(\pi - k_\perp, k_\perp)$.
27. T. Ishiguro, K. Yamaji, *Organic Superconductors*, Vol. 88 of *Springer-Verlag Series in Solid-State Science* (Springer-Verlag, Berlin, Heidelberg, 1990).
28. Pair vertex corrections are present in the 1D regime which yield $z_{\mu,(\bar{\mu})} > 1$ at E_x. Correlations effects are not only present in the Peierls channel but also in the interchain Cooper channel – albeit much weaker in amplitude in the latter case (see references [25,11]).
29. K. Yamaji, J. Phys. Soc. Jpn **52**, 1361 (1983).
30. V.P. Mineev, K.V. Samokin, *Introduction to Unconventional Superconductivity* (Gordon and Breach Science Publishers, Amsterdam, 1999).
31. T. Adachi *et al.*, J. Am. Chem. Soc. **122**, 3238 (2000).
32. H. Wilhelm, D. Jaccard, R. Duprat, C. Bourbonnais, D. Jérome, J. Moser, C. Carcel, J.M. Fabre, Eur. Phys. J. B **21**, 175 (2001).
33. P.M. Chaikin, Phys. Rev. Lett. **69**, 2831 (1992).
34. A. Zhelezyak, V. Yakovenko, Synthetic Metals **70**, 1005 (1995).
35. L.P. Gorkov, A.G. Lebed, J. Phys. Lett. France **45**, L433 (1984).
36. M. Héritier, G. Montambaux, P. Lederer, J. Phys. Lett. France **45**, L943 (1984).
37. P. Chaikin, J. Phys. I France **6**, 1875 (1996).